THE ASTROPHYSICAL JOURNAL, 538:127–133, 2000 July 20

CORRELATED INTENSE X-RAY AND TeV ACTIVITY OF MARKARIAN 501 IN 1998 JUNE

R. M. SAMBRUNA,[1] F. A. AHARONIAN,[2] AND H. KRAWCZYNSKI[2] AND
A. G. AKHPERJANIAN,[3] J. A. BARRIO,[4,5] K. BERNLÖHR,[2,6] H. BOJAHR,[7] I. CALLE,[5] J. L. CONTRERAS,[5] J. CORTINA,[5]
S. DENNINGHOFF,[4] V. FONSECA,[5] J. C. GONZALEZ,[5] N. GÖTTING,[6] G. HEINZELMANN,[6] M. HEMBERGER,[2]
G. HERMANN,[2] A. HEUSLER,[2] W. HOFMANN,[2] D. HORNS,[6] A. IBARRA,[5] R. KANKANYAN,[2,3] M. KESTEL,[4]
J. KETTLER,[2] C. KÖHLER,[2] A. KOHNLE,[2] A. KONOPELKO,[2] H. KORNMEYER,[4] D. KRANICH,[4] H. LAMPEITL,[2]
A. LINDNER,[6] E. LORENZ,[4] N. MAGNUSSEN,[7] O. MANG,[8] H. MEYER,[7] R. MIRZOYAN,[4] A. MORALEJO,[5]
L. PADILLA,[5] M. PANTER,[2] R. PLAGA,[4] A. PLYASHESHNIKOV,[2] J. PRAHL,[6] G. PÜHLHOFER,[2]
G. RAUTERBERG,[8] A. RÖHRING,[6] V. SAHAKIAN,[3] M. SAMORSKI,[8] M. SCHILLING,[8]
D. SCHMELE,[6] F. SCHRÖDER,[7] W. STAMM,[8] M. TLUCZYKONT,[6] H. J. VÖLK,[2]
B. WIEBEL-SOOTH,[7] C. WIEDNER,[2] M. WILLMER,[8] AND W. WITTEK[4]
(The HEGRA Collaboration)
AND
L. CHOU,[1] P. S. COPPI,[9] R. ROTHSCHILD,[10] AND C. M. URRY[11]

Received 2000 February 24; accepted 2000 February 28

ABSTRACT

We present exactly simultaneous X-ray and TeV monitoring with *RXTE* and HEGRA of the TeV blazar Mrk 501 during 15 days in 1998 June. After an initial period of very low flux at both wavelengths, the source underwent a remarkable flare in the TeV and X-ray energy bands, lasting for about 6 days and with a larger amplitude at TeV energies than in the X-ray band. At the peak of the TeV flare, rapid TeV flux variability on subhour timescales is found. Large spectral variations are observed at X-rays, with the 3–20 keV photon index of a pure power-law continuum flattening from $\Gamma = 2.3$ to $\Gamma = 1.8$ on a timescale of 2–3 days. This implies that during the maximum of the TeV activity the synchrotron peak shifted to energies $\gtrsim 50$ keV, a behavior similar to that observed during the longer lasting, more intense flare in 1997 April. The TeV spectrum during the flare is described by a power law with photon index $\Gamma = 1.9$ and an exponential cutoff at ~ 4 TeV; an indication for spectral softening during the flare decay is observed in the TeV hardness ratios. Our results generally support a scenario in which the TeV photons are emitted via inverse Compton scattering of ambient seed photons by the same electron population responsible for the synchrotron X-rays. The simultaneous spectral energy distributions can be fit with a one-zone synchrotron self-Compton model assuming a substantial increase of the magnetic field and the electron energy by factors of 3 and 10, respectively.

Subject headings: BL Lacertae objects: individual (Markarian 501) — galaxies: jets — gamma rays: observations — radiation mechanisms: nonthermal — X-rays: galaxies

1. INTRODUCTION

BL Lacertae (BL Lac) objects are radio-loud active galactic nuclei (AGNs) dominated by nonthermal continuum emission from radio up to γ-rays (MeV to TeV energies) from a relativistic jet oriented at small angles to the observer (e.g., Urry & Padovani 1995). While the radio through UV/X-ray continuum is almost certainly due to synchrotron emission from relativistic electrons in the jet (Ulrich, Maraschi, & Urry 1997 and references therein), the origin of the luminous γ-ray radiation from BL Lac objects is still uncertain. Possibilities include inverse Compton scattering of ambient photons off the jet electrons (Maraschi et al. 1992; Sikora, Begelman, & Rees 1994; Dermer et al. 1992) or hadronic processes (e.g., Dar & Laor 1997; Mannheim 1993).

A breakthrough was provided by the discovery of TeV emission from a handful of such sources, all characterized by a synchrotron peak at higher energies (high-energy peaked BL Lac objects, or HBLs). One of these is Mrk 501 ($z = 0.034$). This source came into much attention after it exhibited a prolonged period of intense TeV activity in 1997 (Catanese et al. 1997; Hayashida et al. 1998; Quinn et al. 1999; Aharonian et al. 1997, 1999a, 1999b, 1999c; Djannati-Atai et al. 1999) accompanied by correlated X-ray emission on timescales of days. Interestingly, this exceptional TeV activity was accompanied by unusually hard X-ray emission up to $\gtrsim 100$ keV (Pian et al. 1998a; Catanese et al. 1997; Lamer & Wagner 1998; Krawczynski et al. 2000), unprecedented in this or any other BL Lac object. The hard X-ray spectrum implied a shift toward higher energies of the

[1] Postal address: Pennsylvania State University, Department of Astronomy and Astrophysics, 525 Davey Lab, University Park, PA 16802.
[2] Max-Planck-Institut für Kernphysik, Postfach 103980, D-69029 Heidelberg, Germany.
[3] Yerevan Physics Institute, Alikhanian Br. 2, 375036 Yerevan, Armenia.
[4] Max-Planck-Institut für Physik, Föhringer Ring 6, D-80805 München, Germany.
[5] Universidad Complutense, Facultad de Ciencias Físicas, Ciudad Universitaria, E-28040 Madrid, Spain.
[6] Universität Hamburg, II. Institut für Experimentalphysik, Luruper Chaussee 149, D-22761 Hamburg, Germany.
[7] Universität Wuppertal, Fachbereich Physik, Gauss-Strasse 20, D-42097 Wuppertal, Germany.
[8] Universität Kiel, Institut für Experimentelle und Angewandte Physik, Leibnizstrasse 15-19, D-24118 Kiel, Germany.
[9] Yale University, New Haven, CT 06520-8101.
[10] Center for Astrophysics and Space Sciences, University of California at San Diego, La Jolla, CA 92093.
[11] STScI, 3700 San Martin Drive, Baltimore, MD 21218.

synchrotron peak, usually located at UV/soft X-rays (e.g., Sambruna et al. 1996; Kataoka et al. 1999), by more than 3 decades, persistent over a timescale of $\sim$10 days (Pian et al. 1998a). Further observations with *BeppoSAX* in 1998 April–May and in 1999 May during periods of TeV lower flux showed that the synchrotron peak had decreased to $\sim$20 and 0.5 keV, respectively (Pian et al. 1998b, 1999). These secular variations of the synchrotron peak suggest a powerful mechanism of particle energization, operating over timescales of years.

Because of its bright TeV emission and unusual X-ray spectral properties, we selected Mrk 501 for an intensive monitoring in 1998 June using HEGRA and the *Rossi X-Ray Timing Explorer* (*RXTE*), with a sampling designed to probe correlated variability at the two wavelengths on timescales of 1 day or shorter. Here we report the first results of the campaign, which is characterized by the detection of a strong flare at both TeV and X-ray energies after a period of very low activity. The structure of this paper is as follows. We describe the sampling and the observations in § 2, the X-ray and TeV light curves in § 3.1, and the TeV and X-ray spectra in §§ 3.2–3.3. Implications of the data are discussed in § 4.

2. SAMPLING AND DATA ANALYSIS

The *RXTE* observations of Mrk 501 started 1998 June 14 and ended June 28, with a sampling of once per day. The exposure time, typically 2–7 ks during the first week of observations (as allowed by visibility), decreased to 0.5–1 ks during the latest period of the campaign, due to reduced visibility constraints. The total exposure in 1998 June was 45,184 s. The remaining 134 ks of the total allocated exposure were rescheduled in 1998 July and August; these data will be presented in a future publication together with simultaneous observations at longer wavelengths (Sambruna et al. 2000, in preparation). The HEGRA observations started 1 day earlier and ended 3 days later than *RXTE*, with typical integration times of 1.5–2 hr per night, covering 100% of the *RXTE* exposure.

2.1. *X-Ray Observations*

The *RXTE* data were collected in the 2–60 keV band with the Proportional Counter Array (PCA; Jahoda et al. 1996) and in the 15–250 keV band with the High-Energy X-ray Timing Experiment (HEXTE; Rothschild et al. 1998). For the best signal-to-noise ratio, Standard 2 mode PCA data gathered with the top layer of the operating PCUs 0, 1, and 2 were analyzed. The data were extracted using the script REX, which adopts standard screening criteria; the net exposure after screening in each Good Time Interval ranges from 0.2 to 6 ks (Table 2; see below). The background was evaluated using models and calibration files provided by the *RXTE* GOF for a "faint" source (less than 40 counts s^{-1} per PCU), using PCABACKEST v.2.1b. Light curves were extracted in various energy ranges to study the energy dependence of the flux variability; for simplicity, only the light curves in 2–4 and 10–20 keV (at the two extremes of the total energy range of the PCA) will be shown here.

The HEXTE data were extracted from both clusters for the same time periods as the PCA. Because of the weak nature of the hard X-ray flux, the data were combined into preflare (MJD 50,980–50,988) and flare (MJD 50,989–50,993) time intervals. In addition, the flare interval was further subdivided into the rising portion (MJD 50,989–50,990) and the rest of the flare containing the peak intensity. The source signal is detected to about 50 keV, and we present results from these average spectra only.

Response matrices for the PCA data were created with PCARMF v.3.5. Spectral analysis of the PCA and HEXTE data was performed within XSPEC v.10.0 using the latest released versions of the spectral response files. The fits were performed in the energy ranges 3–20 and 20–250 keV, where the calibrations are best known. The quoted uncertainties on the spectral parameters are 90% confidence for one parameter of interest ($\Delta\chi^2 = 2.7$).

2.2. *TeV Observations*

The HEGRA Cherenkov telescope system (Daum et al. 1997; HEGRA Collaboration et al. 1999) is located on the Roque de los Muchachos on the Canary Island of La Palma (latitude N28°.8, longitude W17°.9, 2200 m above sea level). The Mrk 501 observations described in this paper were taken from 1998 June 14 to July 3 and comprise 49 hr of best quality data. The analysis tools, the procedure of data cleaning and fine tuning of the Monte Carlo simulations, as well as the estimate of the systematic errors on the differential γ-ray energy spectra, were discussed in detail by Aharonian et al. (1999a, 1999b).

The analysis uses the standard "loose" γ/hadron separation cuts which minimize systematic errors on flux and spectral estimates rather than yielding the optimal signal-to-noise ratio. A software requirement necessitated two imaging atmospheric Cherenkov telescopes within 200 m from the shower axis, each with more than 40 photoelectrons per image and a "distance" parameter of smaller than 1°.7. Additionally, only events with a minimal stereo angle larger than 20° were admitted to the analysis. Integral fluxes above a certain energy threshold were obtained by integrating the differential energy spectra above the threshold energy rather than by simply scaling detection rates. By this means, integral fluxes were computed without assuming a certain source energy spectrum. For data runs during which the weather or the detector performance caused a cosmic-ray detection rate deviating only slightly, i.e., less than 15% from the expectation value, the γ-ray detection rates and spectra were corrected accordingly. Spectral results above an energy threshold of 500 GeV were derived from the data of zenith angles smaller than 30° (39 hr of data). The determination of the diurnal integral flux estimates and the search for variability within individual nights use all data.

3. RESULTS

3.1. *Light Curves*

Figure 1 shows the HEGRA and energy-dependent *RXTE* light curves rebinned on 1 day and 5408 s ($\sim$1 orbit), respectively. The PCA light curves were accumulated in the energy ranges 2–4 and 10–20 keV; for an assumed spectrum with a typical $\Gamma_{3-20\ \mathrm{keV}} = 2.3$ (see below), their effective energies are 3 and 16 keV, respectively (not significantly dependent on the slope).

After a period of very low activity at both TeV and X-rays, a strong flare is apparent at all energies starting on day MJD 50,989 and ending on day MJD 50,994. At TeV energies, the flare has a broad base, lasting approximately 6 days, with a narrow "core" superposed, lasting 2 days

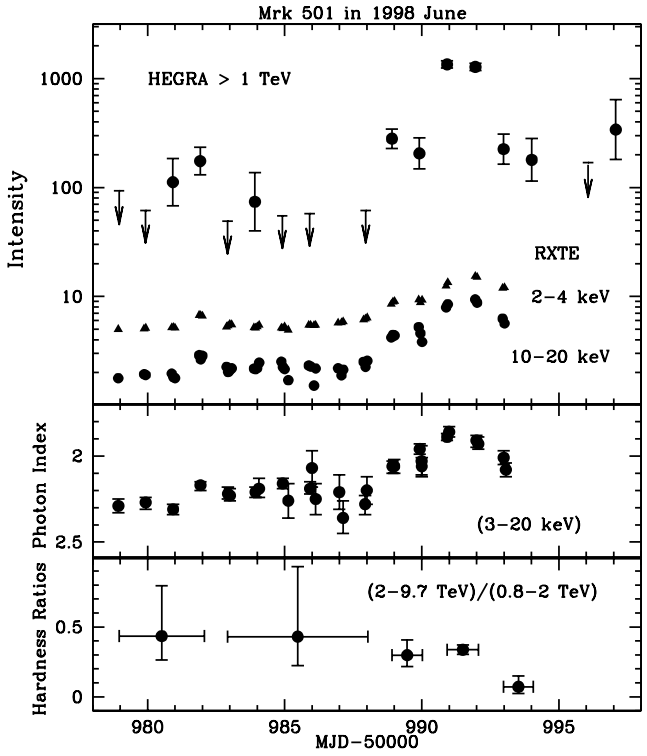

FIG. 1.—Multiwavelength light curves of Mrk 501 in 1998 June, as measured with HEGRA and *RXTE*, binned at 1 day and 5408 s (1 orbit), respectively (*top panel*). The HEGRA flux units are 10^{-12} photons cm^{-2} s^{-1}; the *RXTE* data are in counts s^{-1}. The HEGRA light curve was arbitrarily shifted by +1.5 in logarithmic units for clarity of presentation. A strong flare is detected at both TeV and X-rays, with increasing amplitude for increasing energy. The flare was accompanied by large spectral variations at X-rays (*middle panel*), with flatter slope with increasing flux. Within the statistical errors, the TeV spectrum was rather hard during the whole preflare and flare phases, as shown by the TeV hardness ratios in the bottom panel (upper limits are on 1 σ confidence limit to facilitate the comparison with the error bars of the flux estimates). There is an indication of spectral softening during the decay stage of the flare.

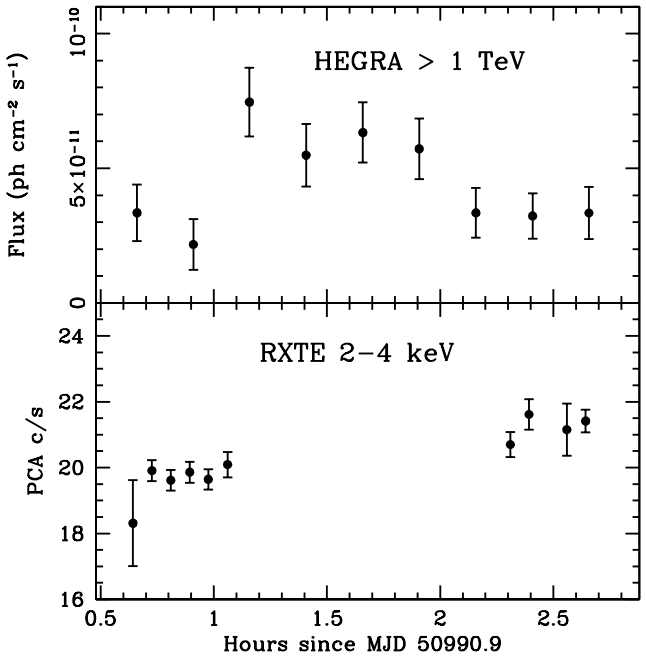

FIG. 2.—TeV and X-ray light curves (binned at 900 and 300 s, respectively) of Mrk 501 during the day of maximum TeV activity in 1998 June. Significant variability of a factor ~2 on a ~20 minute timescale is detected at TeV energies. Unfortunately, gaps are present in the *RXTE* monitoring, and we cannot comment on correlated X-ray variability on these short timescales.

(MJD 50,991–50,992), and a total maximum/minimum amplitude of a factor ~20. The X-rays track well the structure of the TeV flare, although with lower amplitudes (factors of 4 and 2 at hard and soft X-rays, respectively). A correlation analysis using both the discrete correlation function and modified mean deviation methods (Edelson & Krolik 1988; Hufnagel & Bregman 1992) confirm that there are no lags between the TeV and X-ray light curves, or between the soft and hard X-rays, larger than 1 day.

To explore correlations on short timescales, we examined light curves binned at 900 s in TeV and 300 s at X-rays (the best compromise between time resolution and adequate signal-to-noise ratio in both cases). Figure 2 shows the TeV and X-ray light curves for the day of the peak activity, i.e., MJD 50,991, when intrahour variability at TeV energies was detected. The TeV flux varied by a factor of ~2, with the hypothesis of constant flux rejected at the 99.4% confidence level according to the χ^2 test. The doubling timescale of the TeV flux is well below 1 hr (approximately 20 minutes); to our knowledge, this is the shortest flux variability timescale found for Mrk 501 so far (e.g., Quinn et al. 1999) and comparable to Mrk 421 (Gaidos et al. 1996). Unfortunately, as Figure 2 shows, gaps in the *RXTE* sampling prevent us from commenting on subhour correlated variability at X-rays.

A very rapid X-ray flare, with an increase of the 2–10 keV flux by 60% in less than 600 s, was recently detected from Mrk 501 with *RXTE* in 1998 May (Catanese & Sambruna 2000). This result, together with our evidence for fast TeV variability, shows that Mrk 501 can vary on the fastest timescales at both X-ray and TeV wavelengths as other TeV sources (Mrk 421; Maraschi et al. 1999) and calls for future dense X-ray/TeV monitorings aimed at probing correlated variability on the shortest accessible timescales.

3.2. *Simultaneous TeV and X-Ray Spectra*

Because of the sampling, we are able to derive truly simultaneous X-ray and TeV spectra during the preflare and the flare states. The high-state spectra were accumulated during the days of maximum TeV activity, MJD 50,991–50,992, while the preflare spectra were accumulated in the time interval MJD 50,979–50,990. Table 1 reports the results of the spectral fitting of the simultaneous TeV and X-ray spectra, while the data are shown in Figure 3.

The HEGRA spectrum during the flare state was fitted over the energy range from 500 GeV to 20 TeV (above 10 TeV the evidence for emission is only marginal) with a power law plus an exponential cutoff, $dN/dE = N_0 \times (E/\mathrm{TeV})^{-\Gamma} \times e^{(-E/E_0)}$, with spectral parameters reported in Table 1 (with statistical uncertainties). The parameters E_0 and Γ are strongly correlated: within systematic errors the pairs of parameters ($\Gamma = 1.7$; $E_0 = 2.8$ TeV) and ($\Gamma = 2.2$; $E_0 = 6.6$ TeV) are also consistent with the data. Note that the spectral parameters we measure for the 1998 June outburst, i.e., a slope $\Gamma = 1.9$ and cutoff energy $E_0 = 4$ TeV, are very similar to those measured during the 1997 flaring phase (Aharonian et al. 1999a). For the preflare phase, the TeV flux was too low to allow us to fit a power-law model with an exponential cutoff (Table 1). A fit of a power-law

TABLE 1

SIMULTANEOUS AVERAGE TeV AND X-RAY SPECTRA

State[a]	N_0[b]	Γ	E_0 (TeV)	F[c] (10^{-11} ergs cm^{-2} s^{-1})	χ^2_r/dof
TeV:[d]					
Flare	7.9 ± 1.0	1.92 ± 0.3	$4.0^{+1.45}_{-0.90}$	...	0.54/13
Preflare	0.5 ± 0.1	2.31 ± 0.20	...	...	1.4/9
X-ray:[e]					
Flare PCA	...	1.89 ± 0.02	...	18.5 ± 0.9	0.75/42
Flare HEXTE.....	...	2.19 ± 0.29	...	7.5 ± 1.1	1.04/69
Preflare PCA	...	2.21 ± 0.02	...	0.7 ± 0.1	0.85/41
Preflare HEXTE.....	...	2.30 ± 0.45	...	1.8 ± 0.4	0.87/69

[a] High state corresponds to the time interval MJD 50,991–50,992. Low state corresponds to MJD 50,979–50,987.

[b] Normalization of the power law, in 10^{-11} photons cm^{-2} s^{-1} TeV^{-1} for the HEGRA data.

[c] Observed flux in 2–10 keV (PCA) and 20–50 keV (HEXTE).

[d] Fits with a power law plus exponential cutoff: $dN/dE = N_0 \times (E/\mathrm{TeV})^{-\Gamma} \times e^{(-E/E_0)}$. Errors on parameters are statistical.

[e] Fits with a single power law plus Galactic absorption, $N_H = 1.73 \times 10^{20}$ cm^{-2} (Elvis et al. 1989).

model to the ratio of the flare and the preflare spectra gives $(dN/dE)_{\mathrm{flare}}/(dN/dE)_{\mathrm{preflare}} \propto E^{\beta}$ with $\beta = -0.17 \pm 0.19$, consistent within statistics with no spectral evolution.

The PCA spectra were fitted with a single power law with Galactic absorption, 1.73×10^{20} cm^{-2} (Elvis, Lockman, & Wilkes 1989). As can be seen from Table 1, this model provides an excellent fit to the X-ray spectra up to 20 keV, with the photon index flattening from $\Gamma_{3-20\,\mathrm{keV}} = 2.21$ during the preflare state to $\Gamma_{3-20\,\mathrm{keV}} = 1.89$ during the flare. No spectral breaks are required; i.e., there is no statistical improvement when a second power law is added to the fit. However, we cannot exclude the presence of a spectral break at energies softer than sampled with the PCA, $\sim$1–2 keV, as indeed detected with *BeppoSAX* (Pian et al. 1998a).

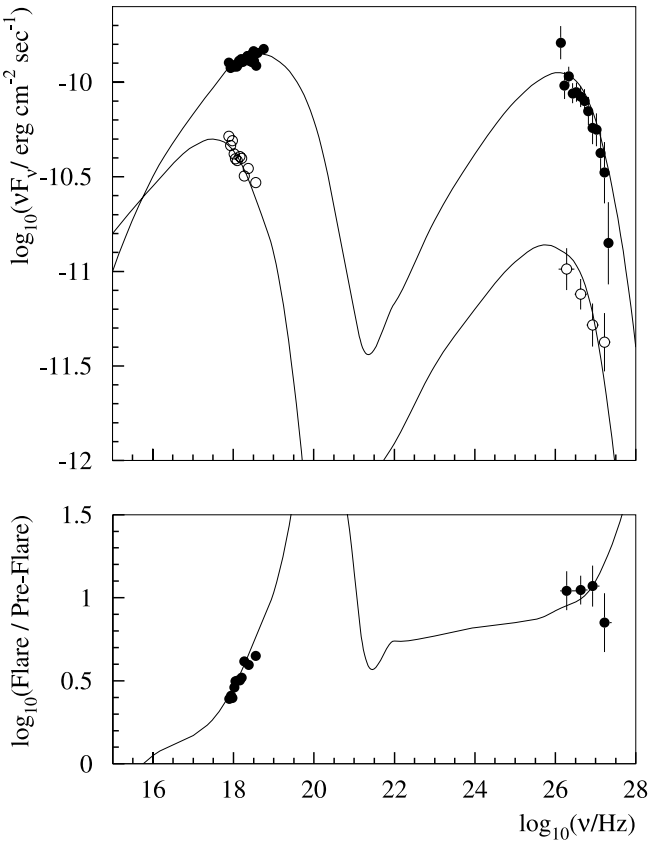

FIG. 3.—Spectral energy distributions of Mrk 501 in 1998 June during the peak of the TeV/X-ray flare (*filled circles*) and during the preflare state (*open circles*). Only the PCA data are plotted for clarity (Table 1). The solid lines are fits to the spectra with a homogeneous SSC model (Coppi 1992) with the following fitted parameters: $B = 0.03$ G, $E_{\mathrm{max}} = 2$ TeV, and $R = 4 \times 10^{16}$ cm for the preflare state; $B = 0.1$ G, $E_{\mathrm{max}} = 20$ TeV, and $R = 2.7 \times 10^{15}$ cm for the high state. The bottom panel shows the ratios of the model spectra and data for the flare and preflare states.

The HEXTE data are fitted by a power law with a photon index consistent with the extrapolation of the PCA slope in both high and low states (Table 1). Indeed, fitting the PCA and HEXTE data sets together, we find that a single power law with a slope similar to the PCA slope describes well the 3–50 keV continuum during both the preflare and flare epochs. Given the large uncertainties of the HEXTE data, however, we cannot rule out the presence of spectral breaks at energies $\gtrsim$10–20 keV, as indeed detected by *BeppoSAX* (Pian et al. 1998a, 1998b).

3.3. *X-Ray and TeV Spectral Variability*

We accumulated time-resolved PCA spectra for each data point of the X-ray light curves in Figure 1 and fitted them over the energy range 3–20 keV with a single power law plus Galactic absorption. The results of the fitting are reported in Table 2 (cols. [3]–[5]), together with the date of the spectrum (col. [1]) and its net exposure (col. [2]). The time progression of the PCA slope is plotted in Figure 1 (*middle panel*). Large variability is readily apparent, with the photon index flattening from $\Gamma_{3-20\,\mathrm{keV}} \sim 2.3$ to $\Gamma_{3-20\,\mathrm{keV}} \sim 1.8$ with increasing flux. There is an indication that the X-ray continuum steepens during the decay stage of the flare.

The X-ray spectral variations follow a well-defined pattern with the intensity. This is illustrated in Figure 4, where the 3–20 keV photon index is plotted versus the 2–10 keV flux. The dotted lines mark the time progression of the slope during the flaring activity and clearly show a "clockwise" loop. This is similar to what was observed in other HBLs (PKS 2005−489: Perlman et al. 1999; PKS 2155−304: Sembay et al. 1993, Sambruna 1999; Mrk 421: Takahashi et al. 1996) and can be interpreted in terms of cooling of the synchrotron-emitting electrons in the jet (Kirk, Riegler, & Mastichiadis 1998).

TABLE 2

X-RAY SPECTRAL VARIABILITY

Start Date (MJD − 50,000) (1)	Net Exposure (s) (2)	$\Gamma_{3-20\,\mathrm{keV}}$ (3)	χ_r^2 (for 42 dof) (4)	$F_{2-10\,\mathrm{keV}}$ (10^{-11} ergs cm^{-2} s^{-1}) (5)
978.9	3168	2.29 ± 0.04	0.55	5.91
979.9	3312	2.27 ± 0.04	0.72	6.05
980.9	6304	2.31 ± 0.03	0.57	6.04
981.9	6320	2.17 ± 0.03	0.84	7.13
982.9	3488	2.22 ± 0.04	0.66	6.29
983.0	4144	2.23 ± 0.04	0.46	6.41
983.9	6192	2.21 ± 0.03	0.73	8.41
984.0	1328	2.19 ± 0.06	0.70	6.58
984.9	5040	2.16 ± 0.03	0.70	6.08
985.1	464	2.26 ± 0.10	0.68	6.02
985.9	3024	2.19 ± 0.04	0.71	6.47
986.0	352	2.07 ± 0.11	0.77	6.43
986.1	528	2.25 ± 0.09	0.78	6.45
986.9	384	2.21 ± 0.10	0.68	6.71
987.1	480	2.36 ± 0.10	0.78	6.76
987.9	1536	2.28 ± 0.06	1.04	7.05
988.0	592	2.20 ± 0.08	0.71	7.29
988.9	1152	2.06 ± 0.04	0.71	10.8
989.0	912	2.06 ± 0.04	0.60	11.4
989.9	1296	1.96 ± 0.03	0.65	12.1
990.0	208	2.03 ± 0.08	0.52	11.3
990.0	512	2.06 ± 0.06	0.74	11.3
990.9	1392	1.89 ± 0.02	1.46[a]	16.9
991.0	656	1.86 ± 0.03	0.99	18.1
991.9	432	1.91 ± 0.03	0.52	20.5
992.0	512	1.93 ± 0.04	0.65	20.0
992.9	528	2.01 ± 0.04	0.47	15.4
993.0	736	2.08 ± 0.04	0.82	15.4

NOTE.—Fits to the PCA data in 3–20 keV with a single power law plus Galactic absorption ($N_H = 1.73 \times 10^{20}$ cm^{-2}). Errors are 90% confidence for one parameter of interest ($\Delta\chi^2 = 2.7$).

[a] High χ^2 is due to instrumental absorption features in the residuals around 4.8 keV (xenon edge) and 8.5 keV (unknown origin).

The HEXTE spectrum accumulated at the beginning of the flare (see § 2) is fitted by a power law with slope $\Gamma_{20-50\,\mathrm{keV}} = 2.19 \pm 0.59$ and 20–50 keV flux $F_{20-50\,\mathrm{keV}} = (5.3 \pm 1.6) \times 10^{-11}$ ergs cm^{-2} s^{-1}. During the peak and decreasing flare, $\Gamma_{20-50\,\mathrm{keV}} = 1.86 \pm 0.28$ and $F_{20-50\,\mathrm{keV}} = (1.1 \pm 0.2) \times 10^{-10}$ ergs cm^{-2} s^{-1}. Comparing to the preflare flux from Table 1, the source brightened by a factor of ~ 6 during the TeV flare in the HEXTE band, with an indication of a hardening of the 20–50 keV continuum.

At TeV energies, given the limited signal-to-noise ratio in the preflare state, we investigated spectral variations by constructing hardness ratios. These are defined as the ratios of the flux in 2–9.7 TeV to the flux in 0.8–2 TeV (the lower bound is chosen to assure negligible systematic errors due to threshold effects, and 2 TeV approximately equals the median energy of photons with energies above 0.8 TeV). The TeV hardness ratios are plotted versus the observation date in Figure 1 (*bottom panel*), together with 1 σ uncertainties. It is apparent that, within statistical uncertainties, the hardness ratios in the preflare state (MJD 50,979–50,990) and flare state (MJD 50,991–50,992) are very similar, despite the fact that the absolute fluxes differ by 1 order of magnitude. Intriguingly, the spectrum seems to soften substantially during the decay stage, although the limited statistical significance of about 2 σ prevents us from drawing firmer conclusions.

4. DISCUSSION

Since the typical flux variability timescale of Mrk 501 in TeV γ-rays and X-rays can be much less than 1 day, it is important to have truly simultaneous observations in both bands. It is also important to have reasonably continuous sampling on timescales of at least 1 day in order to have an accurate picture of the dynamics of the source. For this reason, we conducted a 15 day TeV/X-ray monitoring with diurnal *RXTE* observations exactly in the HEGRA visibility windows. After 10 days of quiescence, the source exhibited a strong flare at both TeV and X-rays lasting 6 days, with a flux exceeding the preflare level by a factor of ~ 20 at TeV energies during a 2 day maximum and with lower amplitudes (factor of 2–4) at X-rays. We also report the first detection of TeV flux variability on subhour timescales in Mrk 501 (§ 3.1).

By chance, our multiwavelength campaign in 1998 June coincided with the only high TeV activity of the source during that year. Luckily, we were able to follow the evolution of the TeV flare not only during the preflare and flare stages but also during the decay stage. The TeV spectrum during the flare is similar to the spectra observed in 1997, suggesting that the flaring episode we witnessed in 1998 June was a scaled-down version of the longer lasting 1997 flare. This conclusion is bolstered by the strong spec-

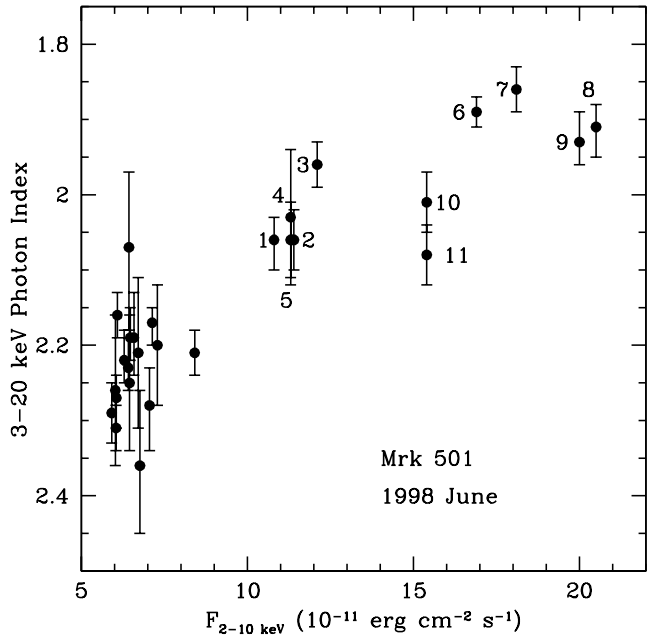

FIG. 4.—Plot of the X-ray 3–20 keV slope vs. the observed 2–10 keV flux, from fits to the time-resolved PCA spectra (Table 2). The trend of flattening slope with increasing flux is apparent. The dotted lines mark the time progression of the slope, which appears to follow a "clockwise" pattern during the flare. This behavior is consistent with the X-ray flare being due to electron cooling (Kirk et al. 1998).

tral variations we observe in the X-rays. Our *RXTE* observations show that the X-ray continuum in 3–20 keV flattened by $\Delta\Gamma_{3-20\ keV} \sim 0.5$ from the beginning of the campaign ($\Gamma_{3-20\ keV} = 2.3$) to the flare maximum ($\Gamma_{3-20\ keV} = 1.8$). Interestingly, at the peak of the TeV flare the X-ray slope was similar to the 2–10 keV slope measured in 1997 April, May, and July with *BeppoSAX* and *RXTE* (Pian et al. 1998a; Lamer & Wagner 1998; Krawczynski et al. 2000). This implies a similar shift of the synchrotron peak frequency at higher energies, $\gtrsim 50$ keV (Fig. 3). While in 1997 April the X-ray continuum flattened by 0.4 within approximately 2 weeks, we see here a comparable flattening within only $\sim$2–3 days. Note that large changes of the position of the synchrotron peak are relatively rare. Besides Mrk 501, they were observed to date only in two HBLs, 1ES 2344+514 (Giommi, Padovani, & Perlman 2000) and 1ES 1426+428 (Ghisellini, Tagliaferri, & Giommi 1999), but not in Mrk 421, PKS 2155−304, or any other BL Lac object. Our observations provide the first evidence that in Mrk 501 the synchrotron peak may change on relatively short timescales ($\sim$a few days).

Several models have been suggested to explain the TeV radiation from blazars. A popular scenario is the leptonic models, where TeV γ-rays are produced via inverse Compton scattering of directly accelerated electrons on external and/or internal photons (e.g., Sikora 1997). For Mrk 501, an object without strong broad-line emission, the synchrotron self-Compton (SSC) model is almost commonly accepted as the most probable explanation for the observed X-ray/TeV–γ-ray emission (e.g., Tavecchio, Maraschi, & Ghisellini 1998; Kataoka et al. 1999). Presently, the SSC model is the only model (at least in its simplified "one-zone" version) that has been developed to a level that allows conclusive predictions that can be compared with experimental results. In particular, the SSC scenario is able to give satisfactory fits to both the X-ray and the TeV spectra (Pian et al. 1998a; Hillas 1999; Krawczynski et al. 2000). We used the code developed by Coppi (1992) to fit our simultaneous spectral energy distributions in Figure 3, assuming emission from a one-zone, homogeneous region and incorporating Klein-Nishina effects. The key parameters used in this model are the Doppler factor δ_j of the relativistic plasma, the radius R of the emission region, the magnetic field B, and the electrons' maximum energy E_{max}.

The results of the fits are shown in Figure 3 as solid lines, and the parameters' values are reported in the caption. As discussed further below, the models were computed without correcting for the extragalactic extinction of TeV photons due to γ-γ pair production with the photons of the diffuse extragalactic background radiation (e.g., Gould & Schréder 1966). In the lower panel, we plot the ratio of the data and best-fit model between the high state and preflare. The latter plot emphasizes that, while the TeV spectra of both states are quite similar, the X-ray spectra of the preflare and the flare state are significantly different. In SSC models, the hardening of the X-ray spectrum during the flare can be attributed to a shift of the peak frequency ν_s of the synchrotron radiation, $\nu_s \propto B \times E_{max}^2$. Assuming an increase of both the magnetic field and the maximum energy during the flare, the dramatic changes of the X-ray spectrum are readily explained (see Fig. 3). While the increase of magnetic field does not affect the γ-ray spectrum, the increase of E_{max} does make the inverse Compton (IC) spectrum harder. However, since the γ-rays are produced in the Klein-Nishina regime, this effect is less pronounced in IC than in the synchrotron radiation component. The fits shown in Figure 3 correspond to the following model parameters: $B = 0.03$ G, $E_{max} = 2$ TeV (exponential cutoff energy), and $R = 4 \times 10^{16}$ cm for preflare state and $B = 0.1$ G, $E_{max} = 20$ TeV, and $R = 2.7 \times 10^{15}$ cm for the flare state. For both cases, a Doppler factor of $\delta_j = 25$ is assumed. Note that the latter value of the Doppler factor implies that internal absorption of the TeV γ-rays by lower frequency photons can be completely neglected (e.g., Celotti, Fabian, & Rees 1998). Furthermore, the chosen Doppler factor and radius of the emitting volume in the flaring state imply time variability down to $t = R/(c\delta_j) = 1$ hr, which agrees with the observed flux variability following from Figure 2. For the flare state with good statistics up to $\sim$10 TeV, the model overpredicts the TeV flux above $\sim$5 TeV, in particular, by a factor of $\sim$2.5 at 10 TeV. This discrepancy should not be overemphasized but could well be the result of intergalactic extinction due to γ-γ pair production.

In summary, we have performed a 2 week monitoring campaign of the HBL Mrk 501 in 1998 June with HEGRA and *RXTE*, with a sampling designed to probe TeV/X-ray correlation on timescales of several hours. We detected a strong flare at both wavelengths, rising from a period of very low activity, well correlated at TeV and X-rays on timescales of $\lesssim$1 day, accompanied by large ($\Delta\Gamma_{3-20\ keV} \sim 0.5$) spectral variability at X-rays. Our results support an interpretation in terms of a canonical synchrotron self-Compton scenario. Future campaigns with a more intensive sampling designed to probe correlation on shorter timescales at both X-ray and TeV energies are needed to set more stringent constraints on the radiative processes that play an important role in the evolution of the flare.

R. M. S. acknowledges support from NASA contract NAS-38252 and NASA grant NAG-7121. R. R. acknowledges support by NASA contract NAS 5-30720. We are grateful to the *RXTE* team, especially Evan Smith, for making these observations possible; to the *RXTE* GOF for constant support with the data analysis; and to Joe Pesce for a careful reading of the manuscript. HEGRA is supported by the German Ministry for Research and Technology (BMBF) and the Spanish Research Council CICYT. We thank the Instituto de Astrophysìca de Canarias for supplying excellent working conditions at La Palma. HEGRA gratefully acknowledges the technical support staff of the Heidelberg, Kiel, Munich, and Yerevan Institutes.

REFERENCES

Aharonian, F. A., et al. 1997, A&A, 327, L5
———. 1999a, A&A, 342, 69
———. 1999b, A&A, 349, 11
———. 1999c, A&A, 349, 29
Catanese, M., et al. 1997, ApJ, 487, L143
Catanese, M., & Sambruna, R. M. 2000, ApJ, 534, L39
Celotti, A., Fabian, A. C., & Rees, M. 1998, MNRAS, 293, 239
Coppi, P. S. 1992, MNRAS, 258, 657
Dar, A., & Laor, A. 1997, ApJ, 478, L5
Daum, A., et al. 1997, Astropart. Phys., 8, 1
Dermer, C. D., et al. 1992, A&A, 256, L27
Djannati-Atai, A., et al. 1999, A&A, 350, 17
Edelson, R. A., & Krolik, J. H. 1988, ApJ, 333, 646
Elvis, M., Lockman, F. J., & Wilkes, B. J. 1989, AJ, 97, 777
Gaidos, J. A., et al. 1996, Nature, 383, 319
Ghisellini, G., Tagliaferri, G., & Giommi, P. 1999, IAU Circ. 7116
Giommi, P., Padovani, P., & Perlman, E. 2000, MNRAS, in press (astro-ph/9907377)
Gould, J., & Schréder, G. 1966, Phys. Rev. Lett. 16, 252
Hayashida, N., et al. 1998, ApJ, 504, L71
HEGRA Collaboration, et al. 1999, Astropart. Phys., 10, 275
Hillas, A. M. 1999, Astropart. Phys., 11, 27
Hufnagel, B. R., & Bregman, J. N. 1992, ApJ, 386, 473
Jahoda, K., Swank, J. H., Giles, A. B., Stark, M. J., Strohmayer, T., Zhang, W., & Morgan, E. H. 1996, Proc. SPIE, 2808, 59
Kataoka, J., et al. 1999, ApJ, 514, 138
Kirk, J. G., Riegler, F. M., & Mastichiadis, A. 1998, A&A, 333, 452
Krawczynski, H., Coppi, P., Maccarone, T., & Aharonian, F. A. 2000, A&A, 353, 97
Lamer, G., & Wagner, S. J. 1998, A&A, 331, L13
Mannheim, K. 1993, A&A, 269, 67
Maraschi, L., et al. 1992, ApJ, 397, L5
———. 1999, ApJ, 526, L81
Perlman, E. S., Madejski, G., Stocke, J. T., & Rector, T. A. 1999, ApJ, 523, L11
Pian, E., et al. 1998a, ApJ, 492, L17
———. 1998b, in ASP Conf. Ser. 159, BL Lac Phenomenon, ed. L. Takalo & A. Sillanpää (San Francisco: ASP), 180
———. 1999, Proc. of the X-Ray Astronomy 1999 Meeting, Astrophys. Lett. Comm., in press
Quinn, J., et al. 1999, ApJ, 518, 693
Rothschild, R., et al. 1998, ApJ, 496, 538
Sambruna, R. M. 1999, in Proc. Frascati Workshop, Vulcano meeting on High-energy cosmic sources, ed. F. Giovannelli & L. Sabau-Graziati, Mem. Soc. Astron. Italiana, in press (astro-ph/9912060)
Sambruna, R. M., Maraschi, L., & Urry, C. M. 1996, ApJ, 463, 444
Sembay, S., et al. 1993, ApJ, 404, 112
Sikora, M. 1997, in AIP Conf. Proc. 410, Proc. Fourth Compton Symp., ed. C. Dermer, M. Strickman, & J. Kurfess (New York: AIP), 494
Sikora, M., Begelman, M., & Rees, M. 1994, ApJ, 421, 153
Takahashi, T., et al. 1996, ApJ, 470, L89
Tavecchio, F., Maraschi, L., & Ghisellini, G. 1998, ApJ, 509, 608
Ulrich, M.-H., Maraschi, L., & Urry, C. M. 1997, ARA&A, 35, 445
Urry, C. M., & Padovani, P. 1995, PASP, 107, 803